

A new large canopy-dwelling species of *Phyllodytes* Wagler, 1930 (Anura, Hylidae) from the Atlantic Forest of the state of Bahia, Northeastern Brazil

Iuri R. Dias¹, Gabriel Novaes-e-Fagundes¹, Antonio Mollo Neto², Juliana Zina³, Caroline Garcia³, Renato Sousa Recoder², Francisco Dal Vechio², Miguel Trefaut Rodrigues² and Mirco Solé^{1,4}

¹ Programa de Pós-Graduação em Zoologia, Universidade Estadual de Santa Cruz, Ilhéus, Bahia, Brazil

² Instituto de Biociências, Universidade de São Paulo, São Paulo, São Paulo, Brazil

³ Departamento de Ciências Biológicas, Universidade Estadual do Sudoeste da Bahia, Jequié, Bahia, Brazil

⁴ Herpetology Section, Zoologisches Forschungsmuseum Alexander Koenig, Bonn, Germany

ABSTRACT

The known diversity of treefrogs of the genus *Phyllodytes* has rapidly increased in recent years, currently comprising 14 species. Recent field work in the Atlantic Rainforest of the state of Bahia lead to the discovery of a new large species of *Phyllodytes* which is herein described based on multiple evidence including morphological, acoustical and genetic data. *Phyllodytes* sp. nov. is one of the largest species within the genus and presents immaculate yellowish dorsum and limbs. The advertisement call of the species is composed of 7–31 notes (half pulsed/pulsatile-half harmonic) with frequency-modulated harmonics. *Phyllodytes* sp. nov. has a karyotype of $2n = 22$ chromosomes, as also found in other species of the genus. Genetic distance values of the 16S mitochondrial rRNA among *Phyllodytes* sp. nov. and its congeners range between 6.4 to 10.2%. The description of another new species for this state reinforces the need for further taxonomic work with *Phyllodytes* in this region that has been revealed as a priority area for research and conservation of this genus.

Submitted 18 September 2019

Accepted 27 January 2020

Published 23 June 2020

Corresponding author

Iuri R. Dias, iurirdias@hotmail.com

Academic editor

Max Lambert

Additional Information and
Declarations can be found on
page 20

DOI 10.7717/peerj.8642

© Copyright
2020 Dias et al.

Distributed under
Creative Commons CC-BY 4.0

OPEN ACCESS

Subjects Biodiversity, Taxonomy, Zoology

Keywords Amphibia, Biodiversity, Bromeliad, Integrative taxonomy, Lophyohylini

INTRODUCTION

The genus *Phyllodytes* Wagler, 1830 assembles 14 species, distributed mainly throughout the morphoclimatic domain of the Atlantic Forest, most of them with occurrence in the northeast of Brazil (Orrico, Dias & Marciano-Jr, 2018; Frost, 2019;). These small to medium-sized tree frogs (18.2–48.5 mm SVL) are characterized mainly by the presence of odontoids on their mandibles and association with bromeliads, where they complete their entire life cycle (Bokermann, 1966; Peixoto, 1995; Cruz, Feio & Cardoso, 2006).

Although some species of *Phyllodytes* can use terrestrial bromeliads (Ferreira, Schineider & Teixeira, 2012; Cunha & Napoli, 2016), most calling males are heard from bromeliads in the forest canopy, hampering the sampling of representatives of this genus. Thus, this peculiar life history trait may explain the scarcity of studies dealing with its taxonomy,

ecology and phylogeny (*Marciano-Jr, Lantyer-Silva & Solé, 2017*). Fortunately, this scenario is changing due to the greater attention that the genus has received recently, with half of the species within the genus (i.e., seven species) having been described in the last 15 years (*Frost, 2019*).

The state of Bahia is a diversity hotspot for *Phyllodytes* with nine of the 14 known species (*Orrico, Dias & Marciano-Jr, 2018*). Notwithstanding, these numbers may underestimate the actual number of species as inventories carried out in coastal areas of the south of the state indicate difficulties in assigning species names to collected individuals (*Dias et al., 2014; Dias, Mira-Mendes & Solé, 2014; Mira-Mendes et al., 2018*), suggesting that the diversity within the genus may be even larger. This assumption has been corroborated by the description of three new endemic species from southern Bahia in the last three years (*Marciano-Jr, Lantyer-Silva & Solé, 2017; Vörös, Dias & Solé, 2017; Orrico, Dias & Marciano-Jr, 2018*).

During recent field trips to the Atlantic Forest of southern Bahia we collected specimens of *Phyllodytes* (adults and tadpoles) from both terrestrial and epiphytic bromeliads. A closer examination revealed that these specimens correspond to an undescribed species. Herein, we describe this new species based on morphology of adults and tadpoles, bioacoustics, cytogenetic and molecular evidence. In addition, we compile and discuss available information on bioacoustic features and tadpole morphology of the genus.

MATERIALS & METHODS

Morphological data

We analyzed specimens housed at herpetological collections of Museu de Zoologia da Universidade Estadual de Santa Cruz, Ilhéus, state of Bahia, Brazil (MZUESC), Museu de História Natural de Jequié, Coleção Herpetológica, Jequié, state of Bahia, Brazil (MHNJCH) and Museu de Zoologia da Universidade de São Paulo, state of São Paulo, Brazil (MZUSP). Examined specimens are listed in [Appendix 1](#). For comparisons with *Phyllodytes brevirostris*, *P. edelmoi* and *P. gyrinaethes*, we used data available in the literature (*Peixoto & Cruz, 1988; Peixoto, Caramaschi & Freire, 2003*). Specimens collected for this work were obtained under IBAMA #12920-1 and ICMBIO #13708-1 and #35068 permits. This research was approved by the ethics committee on the use of animals (CEUA-UESC 002/12).

We took the following measurements of adult specimens: SVL (snout-vent length), HL (head length), HW (head width), IND (internarial distance), END (eye-nostril distance), ED (eye diameter), IOD (interorbital distance), TD (tympanum diameter), THL (thigh length), TBL (tibia length), TAL (tarsus length), FL (foot length), HAL (hand length), DF3 (width of disc on finger III) and 4TD (toe IV disc diameter). We measured SVL, HL, HW, THL, TL and FL with calipers to the nearest 0.02 mm. The remaining measurements were made with calipers under a stereo microscope. Measurements followed *Kok & Kalamandeen (2008)* with the exception of IOD that was measured between the anterior corners of the eyes in order to enhance repeatability. Snout profile terminology followed *Heyer et al. (1990)*, texture of dorsal skin is described according to *Kok & Kalamandeen (2008)* and webbing formula notation followed *Savage & Heyer (1967)* and *Savage & Heyer (1997)*,

measured on left hand and foot. Colour in life was described based on photographs of live specimens taken during the day.

Cranial osteology

We scanned two individuals of the new species, one adult (MZUSP 157524) and one juvenile (MZUSP 157526) with a SkyScan digital microtomograph with a resolution of 18 μm and of 9 μm , respectively. The images were processed in CT Analyzer v.1.11 software. The resulting 3D models were visualized on CTvox v.3.3 software, and the osteological descriptions were made based on three-dimensional images. Terminology of osteological elements follows [Trueb \(1973\)](#) and [Duellmann & Trueb \(1986\)](#).

Tadpole

Two tadpoles (MZUSP 157525) of the new species were obtained together with an adult male (MZUSP 157524), in a large bromeliad (ca. 100 cm diameter) on a trunk of a large tree at 8 m height at Estação Ecológica Estadual de Wenceslau Guimarães, Wenceslau Guimarães municipality, State of Bahia, Brazil (13°35'41.8"S, 39°43'10.5"W). Mitochondrial sequences obtained from a piece of the tail fin of one tadpole at stage 27 of [Gosner \(1960\)](#) confirmed their conspecificity (tadpoles obtained with MTR 22178 referred to as *Phyllodytes* sp. 2 in [Blotto et al., 2020](#)). Tadpoles were euthanized in 5% lidocaine, fixed and preserved in 10% formalin. Terminology for external morphology follows [Altig & McDiarmid \(1999\)](#). Tadpole description and illustrations are based on the specimen at developmental stage 35 of [Gosner \(1960\)](#), and compared with the specimen at stage 27.

We measured 13 morphometric variables with a Digimess[®] digital caliper (precision ± 0.01 mm) and a micrometer ocular in a Nikon SMZ645 stereomicroscope following [Altig & McDiarmid \(1999\)](#): total length (TL), body length (BL), body height (BH), body width (BW), interorbital distance (IOD), internarial distance (IND), eye diameter (ED), eye-nare distance (END), nare-snout distance (NSD), tail length (TAL), maximum tail height (MTH), tail muscle height (TMH) and tail muscle width (TMW). The drawings were prepared with the aid of digital photograph obtained with an Olympus DP72 digital camera attached to an Olympus SZX12 stereomicroscope.

Bioacoustic data

We recorded the advertisement call of two individuals at their natural habitat before collecting. The holotype was recorded with a digital recorder (Tascam DR1) with a directional microphone (Sennheiser ME45), on March 2nd 2015, between 00:40 am–02:00 am, at a distance of ~ 0.5 m and air temperature of 21.9 °C. The animal was calling from a terrestrial bromeliad and no conspecifics were heard nearby. For the analysis of notes, we used only the notes from 10 randomly selected calls.

One paratype (MZUESC 18265) was recorded with a digital recorder (Marantz PMD660) with a shotgun microphone (Sennheiser-ME66), on June 18th 2014, around 00:10 am, at a distance of ~ 1 m and air temperature of around 19 °C. The animal was calling from an isolated epiphytic bromeliad (*Hohenbergia* sp.) around 3.1 m above the ground. During the recording, we imitated the frog call (“vocal playback”) to stimulate its response. For this reason, we did not measure the interval between calls, as they would be uninformative.

In eight occasions the male emitted a different type of call, which we named “call type II”. We deposited all recordings at the Fonoteca Neotropical Jacques Vielliard (FNJV 40997, 41382–41384).

All callings were recorded in uncompressed PCM format with a sample rate of 44.1 kHz and 16 bits. Sound analysis was made with Raven Pro 1.4. Time components were measured from the waveform, while spectral components were measured from the spectrogram. We set the spectrographic parameters as following: window type: Hann, window size: 1024 samples, 3dB filter bandwidth: 61.9 Hz, time grid overlap: 90%, time grid size: 102 samples, frequency grid DFT size: 1024 samples, frequency grid spacing: 43.1 Hz. When necessary, we filtered the frequencies below 150 Hz to reduce wind sound interference, and above 5000 Hz, to reduce insect sound interference, using the “Filter out active selection” tool. Categorization of sound types follows [Beeman \(1998\)](#), modified by [Köhler et al. \(2017\)](#). We used a note-centered terminology (*sensu* [Köhler et al., 2017](#)) for the call elements nomenclature.

The following parameters were measured from the calls: call duration (from peak amplitude of the first note to the peak of the last note of each call), interval between calls (from peak amplitude of the last note of a call to the peak amplitude of the first note of next call) and number of notes of the call. For the analysis of the notes we delimited the selection borders of each note using the threshold of 5% of the maximum amplitude of the note (see [Littlejohn, 2001](#)). Based on this selection, the following automated measurements (see [Charif, Waack & Strickman, 2010](#)) were taken: duration 90%, dominant frequency, bandwidth 90%, frequency 5% and frequency 95%. Then, we made additional smaller selections to measure the initial and final frequency of the first harmonic (the peak frequency of the first 0.015 s and of the last 0.015 s of the first harmonic). Finally, we measured the inter-note interval, note emission rate and note shape (note rise time divided by note duration).

For the comparisons with the calls of the congeneric species, we used the data available in the published call descriptions. Based on the literature and our personal observations, we assume functional homology between the herein defined notes and those described for other species of the genus *Phyllodytes*.

Cytogenetic data

We karyotyped one paratype (MZUESC 18265) which was injected with colchicine 0.5% six hours before euthanasia with a lethal dose of lidocaine. Mitotic chromosomes were obtained from intestinal epithelium after 30 min under distilled water and 24 h in cold Carnoy fixer (3:1) following a modified protocol from [King & Rofe \(1976\)](#).

Chromosomic classification followed [Levan, Fredga & Sandberg \(1964\)](#) by adopting the following limits for the Arm Ratio (AR): AR = 1.00 to 1.70, metacentric; AR = 1.71–3.00, submetacentric; AR = 3.01–7.00 subtelocentric; AR = greater than 7.00, acrocentric. They were arranged in decreasing order of size. Metacentric, submetacentric and subtelocentric chromosomes have two arms, the acrocentric ones a single one.

The C-banding was obtained as described by [Sumner \(1972\)](#) with the following modifications: the blades were immersed in HCl 0.2 N for 13 min at room temperature and

then immersed in Ba(OH)₂ solution at 60 °C for 35 s and in 2X SSC at 60 °C for 30 min. Nucleolar organizing regions (NORs) were identified by silver nitrate impregnation following *Howell & Black (1980)* and FISH with 18S rDNA probe according to *Pinkel, Straume & Gray (1986)* and *Hatanaka & Galetti (2004)*.

At least 30 metaphase spreads were analyzed to confirm the 2n and karyotype structure results. Images were captured using an Olympus BX50 microscope (Olympus Corporation, Ishikawa, Japan) with CoolSNAP camera and the images processed using Image Pro Plus 4.1 software (Media Cybernetics, Silver Spring, MD, United States).

Molecular data

We sequenced the final part of fragment of the mitochondrial 16S ribosomal RNA gene (16S rRNA) from the holotype (MZUESC 18264) and from a paratype (MZUESC 18265). We also sequenced the same fragment for one topotype of *Phyllodytes kautskyi* (Museu de Biologia Mello Leitão - MBML 8818) from Domingos Martins, State of Espírito Santo (GenBank: [MN648397–MN648399](#); [Document S1](#)) following protocols of *Faivovich et al. (2005)* and using the primers 16SC (F): 5'-GTRGGCCTAAAAGCAGCCAC-3' (*Darst & Cannatella, 2004*) and 16SBr-H (R): 5'-CCGGTCTGAACTCAGATCACGT-3' (*Palumbi et al., 2001*).

Phylogenetic analyses

Sequence alignment was carried out using the MAFFT algorithm with L-INS-i strategy (*Katoh & Toh, 2008*). Phylogenetic reconstruction was performed using the Bayesian inference with MrBayes 3.2.3 (*Huelsenbeck & Ronquist, 2001*) after the best model of evolution was determined using jModelTest 2.1.3 (*Darriba et al., 2012*) based on Akaike information criterion to be GTR+I+G. Bayesian analyses included two independent runs, each with four chains and sampling every 1000 generations for 70 million generations. We examined trace plots and effective sample size in Tracer 1.7 (*Rambaut et al., 2018*) to check MCMC mixing and convergence. We removed trees from the first 20% of the samples as burn-in. A consensus of the post burn-in trees was visualized in FigTree 1.4.2 (<http://tree.bio.ed.ac.uk/software/figtree>). These analyses were performed at CIPRES Science Gateway (*Miller, Pfeiffer & Schwartz, 2010*). We included homologous sequences available in Genbank of all species of *Phyllodytes* and of at least one species from all genera of Lophyohylini tribe (*sensu Faivovich et al., 2005*). We used Cophomantini *Nesorohyla kanaïma* to root the tree following the results of a previous phylogenetic analysis (*Faivovich et al., 2005*; *Duellman, Marion & Hedges, 2016*). To estimate the genetic distance, we calculated uncorrected p-distances among the species of *Phyllodytes* in MEGA 6.06 (*Tamura et al., 2013*), considering d:transitions + transversions, uniform rates among sites, and gaps/missing data as complete deletion.

Nomenclatural acts

The electronic version of this article in Portable Document Format (PDF) will represent a published work according to the International Commission on Zoological Nomenclature (ICZN), and hence the new names contained in the electronic version are effectively published under that Code from the electronic edition alone. This published work

and the nomenclatural acts it contains have been registered in ZooBank, the online registration system for the ICZN. The ZooBank LSIDs (Life Science Identifiers) can be resolved and the associated information viewed through any standard web browser by appending the LSID to the prefix <http://zoobank.org/>. The LSID for this publication is as follows: urn:lsid:zoobank.org:pub:FD2CACD2-F59F-4B75-947D-B576701424D9. The online version of this work is archived and available from the following digital repositories: PeerJ, PubMed Central and CLOCKSS.

RESULTS

Generic placement.— The new species can be allocated to the genus *Phyllodytes* by the presence of odontoids in the mandible and phylogenetic reconstructions indicate close relationship to other species in this genus also supporting this placement (see below).

Phyllodytes magnus sp. nov.

Phyllodytes kautskyi—(Freitas, 2015)

Phyllodytes cf. *kautskyi*—(Freitas et al., 2018)

urn:lsid:zoobank.org:act:D8DF9024-57C1-413B-9D05-B0CF05B7929C

Holotype.— MZUESC 18264, adult male (Figs. 1, 2, 3A and 3C) found in a terrestrial bromeliad, on March 2nd 2015, by IRD and Carlos Augusto Souza-Costa at Serra da Jibóia (12°52'19.08"S, 39°28'53.90"W; 490 m a.s.l.; WGS84), between the municipalities of Santa Terezinha and Elísio Medrado, State of Bahia, Brazil.

Paratypes.— MZUESC 18265 (ex-MHNJCH 914), adult male (Fig. 3B and 3D), collected in an epiphytic giant bromeliad (*Hohenbergia* sp.) at ~3.10 m above the ground at Parque Estadual da Serra do Conduru (14°29'36.80"S, 39°08'10.70"W; 201 m a.s.l.; WGS84), municipality of Uruçuca, State of Bahia, Brazil, on June 19th 2014, by GNF and Joedison dos Santos Rocha; MZUSP 157524 (adult male) and MZUSP 157526 (juvenile), both collected in Estação Ecológica Estadual de Wenceslau Guimarães (13°35'41.8"S, 39°43'10.5"W; 530 m a.s.l.; WGS84), municipality of Wenceslau Guimarães, State of Bahia, Brazil, on December 14th 2011, by MTR, RSR, Mauro Teixeira Junior and FDV.

Etymology.— The specific epithet is an adjective from Latin meaning “great” or “large” (Lewis & Short, 1891), and refers to the large size of the adult males collected from this species, which are among the largest known in the genus.

Diagnosis.— A large species (SVL 36.4 to 41.1 mm in males, $n = 3$) characterized by (1) snout mucronate in dorsal view, acute in profile; (2) mandible with two anterior large odontoids on each side in adults; (3) adults males with dorsum of body and limbs immaculate, uniformly pale yellow; (4) dorsal skin granular; (5) ventral skin cream and evenly granular, lacking distinct rows of tubercles; (6) a row of tubercles along lateral surface of forearm and tarsus; (7) tubercle subarticular from second segment of finger IV single and rounded shape; (8) canthus rostralis immaculate; (9) tympanum size corresponding to 6.6–7.1% of SVL; (10) advertisement call consisting of a series of 7–31 composite notes (half pulsed/pulsatile–half harmonic).

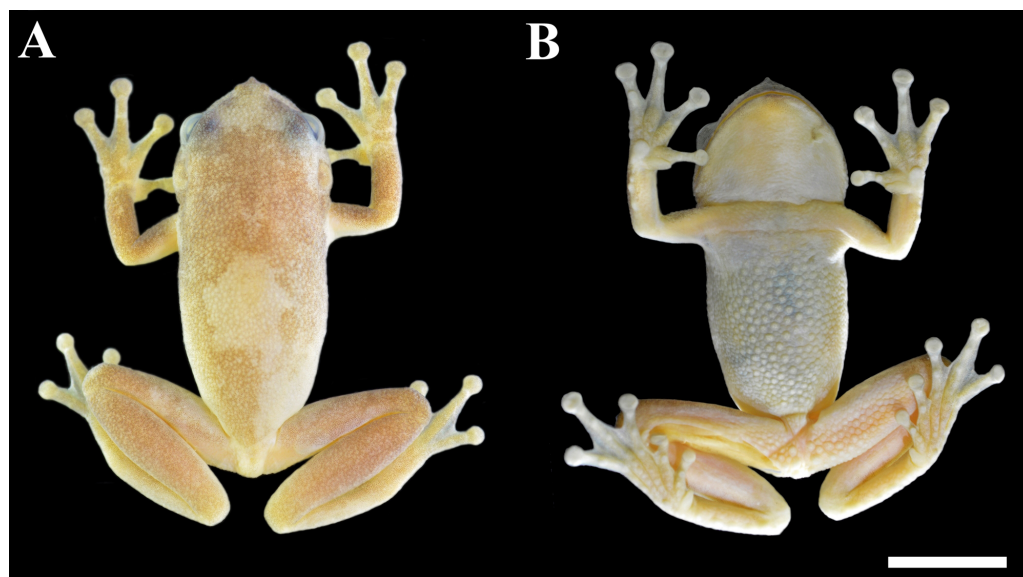


Figure 1 Holotype of *Phyllodytes magnus* sp. nov. (MZUESC 18264; SVL 36.4 mm). (A) Dorsal and (B) ventral view of the body. Scale bar = 10 mm.

Full-size  DOI: [10.7717/peerj.8642/fig-1](https://doi.org/10.7717/peerj.8642/fig-1)

Description of holotype.— An adult male in good state of preservation, with a piece of muscle removed from the right thigh for molecular analyses. Raw measurements are detailed in [Table S1](#). Body robust; head wider than long (HL 89.4% of HW; HW 39.0% of SVL; HL 34.9% of SVL); snout mucronate in dorsal view and acute in profile ([Figs. 1, 2A and 2B](#)); nostrils small, elliptical, directed anterolaterally, nearer to the tip of snout than to eye; *canthus rostralis* slightly concave; loreal region oblique, slightly concave; internarial distance smaller than eye–nostril distance (IND 67.5% of END), eyes large (ED 27.6% of HL; 24.6% of HW; 87.5% of END), prominent, situated laterally, directed anterolaterally; tympanum evident, relatively medium (TD 7.1% of SVL and TD 20.5% of HL), nearly circular, separated from posterior border of eye by approximately the half of diameter of tympanum; tympanum diameter smaller than eye to nostril distance (TD 65% of END), eye diameter (TD 74.3% of ED), interorbital distance (TD 31.3% of IOD); slightly smaller than internarial distance (TD 96.3% of IND), its diameter larger than width of discs on third finger (TD/DF3 = 1.24) and of fourth toe (TD/4TD = 1.36); tympanic annulus evident; supratympanic fold developed, covering dorsal edge of tympanum nearly straight, posteriorly slightly curved downwards and extending until near the insertion of arm; vocal sac single, subgular, poorly developed; vomerine teeth in two patches, oblique and barely separated, positioned below and between choanae; each side of mandible with two large anterior and smaller, discrete and subequal odontoids, pupil horizontal with distinct meniscus.

Arms slightly thicker than forearms (forearm/arm = 94.5%); lateral margin of forearms crenate, with four outer tubercles, those closest to hand, smaller and less evident; hand large ([Fig. 2C](#)), 31.6% of SVL, slightly crenate laterally; fingers, in the following order of length, I < II \cong IV < III; subarticular tubercles rounded, the second of the fourth finger single

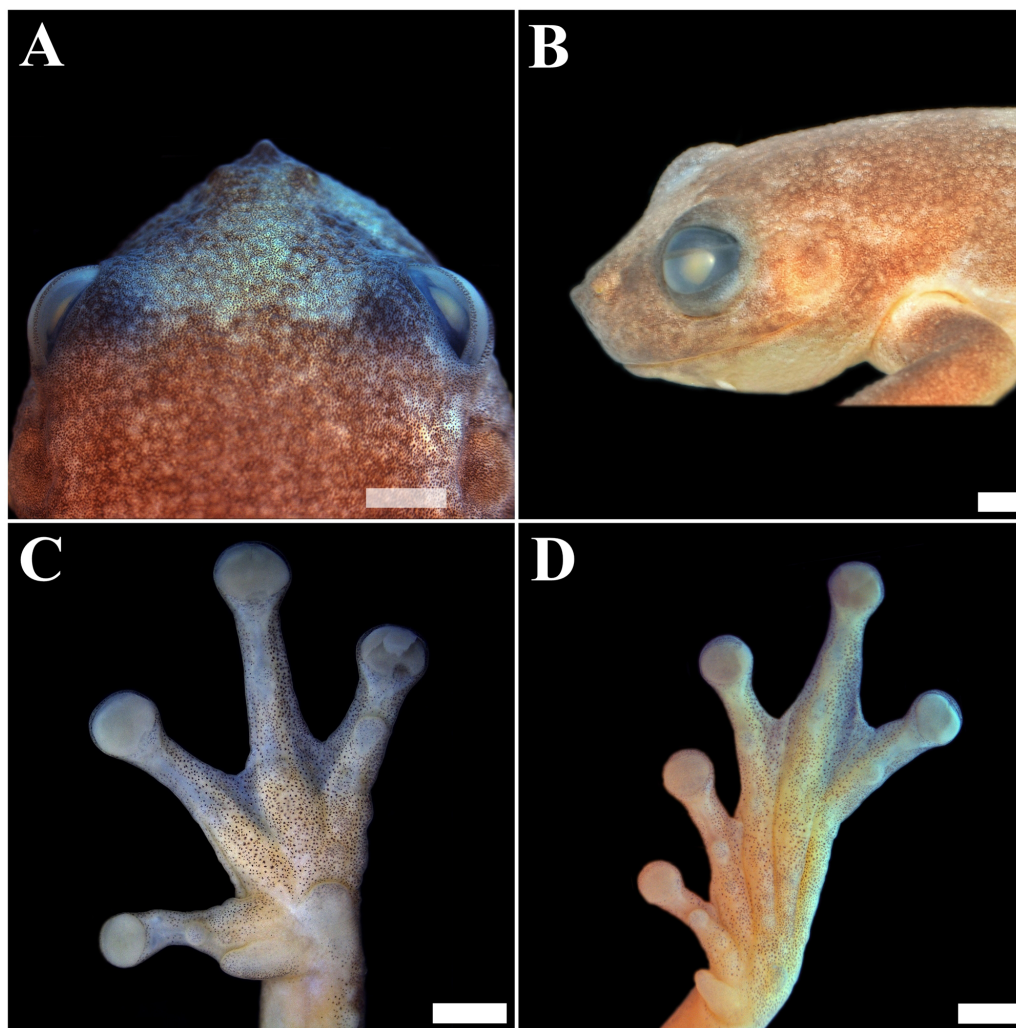


Figure 2 Holotype of *Phyllodytes magnus* sp. nov. (MZUESC 18264). (A) Dorsal view of the head; (B) Lateral view of the head (left side); (C) Plantar view of the left hand and (D) Plantar view of the left foot. Scale bar = two mm.

Full-size  DOI: [10.7717/peerj.8642/fig-2](https://doi.org/10.7717/peerj.8642/fig-2)

(Fig. S1A); a few small supranumerary tubercles; palmar tubercle well developed, rounded; thenar tubercle large, elliptical; adhesive discs developed; first finger's disc smaller, than the others; diameter of disc of third finger equivalent to 60.0% of eye diameter; fingers fringed; webbing formula I –II 2 –3⁺ III 3 –21/2 IV.

Hind limbs long; tibia slightly longer than thigh (THL 95.6% of TBL); sum of tibia and thigh lengths 96.7% of SVL; a row of evident tubercles along lateral surface of tarsus; tarsus length smaller than foot length (TAL 65.1% of FL); foot length smaller than thigh and tibia lengths (FL 84.9% of THL; FL 81.1% of TBL); plantar surface with supernumerary tubercles; subarticular tubercles rounded; inner metatarsal tubercle well developed elongated, projecting laterally; outer metatarsal tubercle small and rounded;

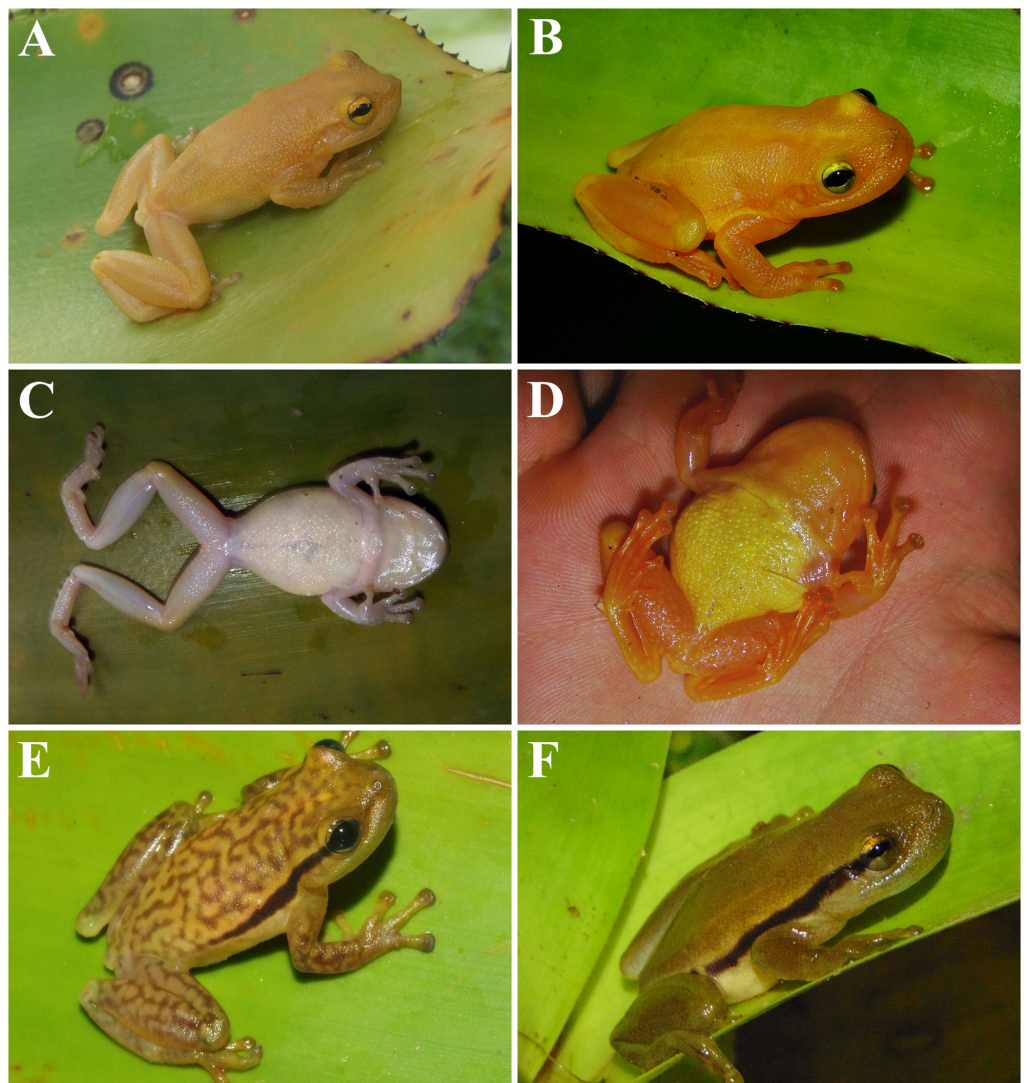


Figure 3 *Phyllodytes magnus* sp. nov. (A, B, C, D), *P. maculosus* (E) and *P. kautskyi* (F) in life.

Phyllodytes magnus sp. nov, holotype (MZUESC 18264) in (A) dorsal and (C) ventral view and paratype (MZUESC 18265) in (B) dorsal and (D) ventral view. In (E) *P. maculosus* and (F) *P. kautskyi*.

Full-size  DOI: 10.7717/peerj.8642/fig-3

discs on toe I slightly smaller than those of other toes; toes fringed; webbing formula I 2⁻–3^{1/2} II 2⁻–3⁺ III 2⁻–3⁺ IV 3⁻–11^{1/2} V.

Dorsal surface of body, forearms, and tibia very granular; belly granular without distinct rows of tubercles; throat, anterior and posterior surfaces of thighs and ventral surface of shanks smooth; ventral surface of thighs granular with distinct round tubercles of which a pair near thigh insertion is more prominent.

Dorsum immaculate, uniformly pale yellow; ventral surface of body, limbs and thighs cream white; iris yellow with black horizontal band projecting from pupil.

Variation.— The measurements of the specimens from the type series are summarized in [Table S1](#). Overall, the type series is morphologically congruent with the holotype. However,

one paratype (MZUESC 18265) shows the following differences: the snout outline is more rounded in dorsal and profile view, because the apical tubercle is less developed and the upper jaw more protruding; in life, the dorsum, the throat and the ventral surfaces of limbs are orange-yellow and the belly is golden-yellow (Figs. 3B and 3D); webbing formula for the left hand is I–II 2[–]–3⁺ III 3–2⁺ IV, and for the left foot is I 2[–]–3 II 11/2–3[–] III 11/2–3[–] IV 21/2–1⁺ V. The juvenile (MZUSP 157526) has black spots on dorsum, which are absent on adults. This suggests that this species passes through ontogenetic pattern change. **Comparisons with congeners.**— *Phyllodytes magnus* is promptly distinguished from most of other congeners by the larger size of its males (36.4–41.1 mm vs. 15.6–28.7 mm), except for *P. maculosus* (39.7–43.5 mm) and *P. kautskyi* (38.0–42.0 mm). The single and rounded shape of the subarticular tubercle in the second segment of finger IV distinguishes *P. magnus* from *P. kautskyi* and *P. maculosus* (tubercles elongated and bifid in these species—Fig. S1). In addition, the dorsal skin is granular in *P. magnus* and smooth or shagreened in *P. maculosus* and *P. kautskyi* (Fig. S2).

The absence of dorsolateral dark stripes distinguishes *Phyllodytes magnus* from *P. amadoi*, *P. kautskyi* (Fig. 3F), *P. luteolus*, *P. maculosus* (Fig. 3E), *P. melanomystax*, *P. praeceptor*, *P. punctatus*, *P. tuberculosus* and *P. wuchereri* (all have a pair of dorsolateral dark stripes extending from the posterior corner of the eyes towards the inguinal region, though the length and density of the stripes varies according to the species). The immaculate dorsum of body and limbs distinguishes *Phyllodytes magnus* from *P. amadoi* and *P. praeceptor* (small, irregular brown patches), *P. gyrinaethes* (dorsal surfaces of body and limbs with marbled pattern), *P. maculosus* (cream colored dorsum with anastomosed brown blotches), *P. melanomystax* (black round spots in the dorsum, not present in all individuals/populations), *P. punctatus* and *P. tuberculosus* (distinctive brown dots on dorsum) and *P. wuchereri* (a pair of dorsolateral longitudinal white stripes and, in some individuals/populations, dorsum of hind limbs and central area of dorsum of body mottled brown).

Phyllodytes magnus like *P. gyrinaethes*, *P. kautskyi*, *P. maculosus* and *P. melanomystax*, has an evenly granular venter without the distinctive rows of ventral tubercles present in *P. acuminatus*, *P. amadoi*, *P. brevirostris*, *P. edelmoi*, *P. luteolus*, *P. megatympanum*, *P. punctatus*, *P. praeceptor*, *P. tuberculosus* and *P. wuchereri*. The immaculate *canthus rostralis* and snout also distinguishes *P. magnus* from *P. melanomystax* (thick dark brown stripe on the snout and *canthus rostralis*). Furthermore, the absence of highlighted color in groin also distinguishes *P. magnus* from *P. megatympanum* (yellow groin) and *P. gyrinaethes* (red groin). In addition, the relative tympanum size corresponding to 6.7–7.1% of SVL distinguishes *P. magnus* from *P. megatympanum* and *P. acuminatus* (TD 7.73–8.16% of SVL).

Cranial osteology.— Dermal roofing bones (Fig. 4A). Skull is broad and relatively flat, wider than long. In dorsal view, nasals paired, trapezoidal, overlying the olfactory region of the skull. Sphenethmoid diamond-shaped, fused anteriorly, with posteromedial margins of nasals, and posteriorly, with anterior margins of frontoparietals. Frontoparietals present, paired, longer than wide, wider anteriorly, constricted medially. The anterior terminus of the pterygoid appears at the first third of the orbit.

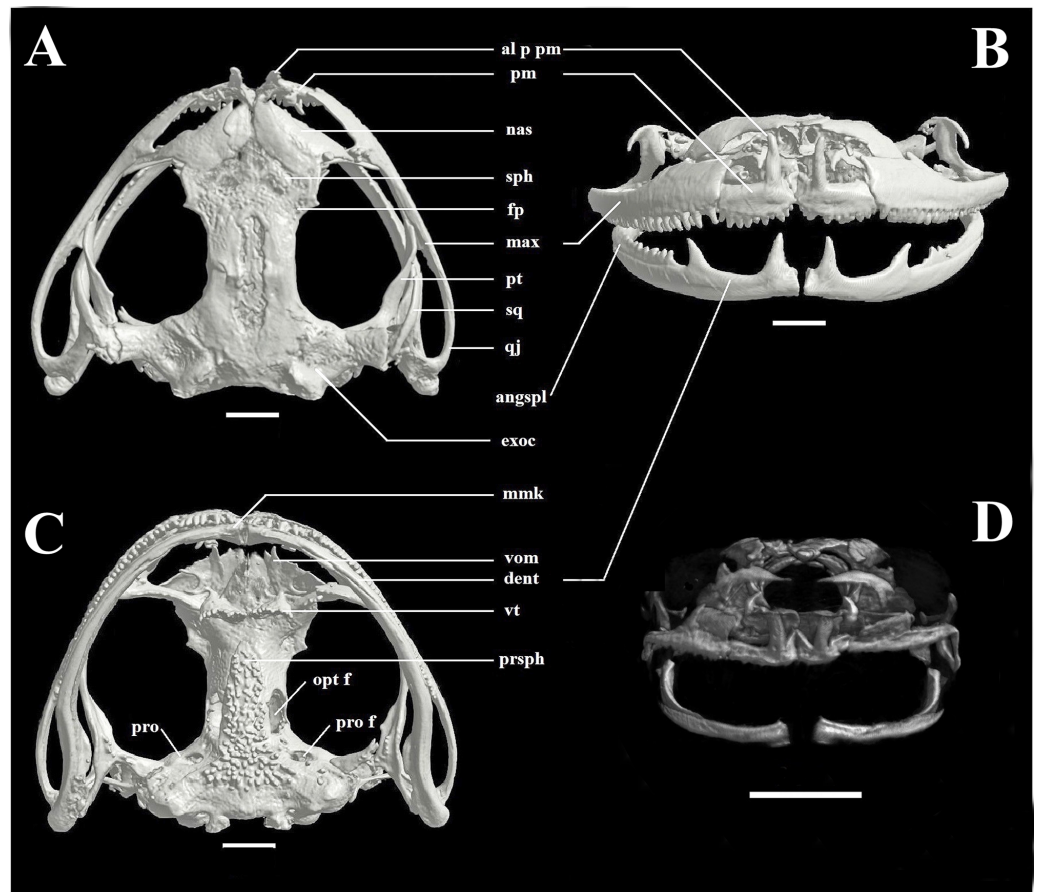


Figure 4 Skull of *Phyllodytes magnus* sp. nov. (A - dorsal, B - ventral and C - front view) = Adult (MZUSP 157524) and (D - front view) = juvenile (MZUSP 157526); Scale bar = two mm. Abbreviations: al p pm, alary process of premaxilla; angspl, angulosphenial; dent, dentary; exo, exoccipital; fp, frontoparietal; max, maxilla; mmk, mentomeckelian bone; nas, nasal; opt f, optic foramen; pm, premaxilla; pro, prootic; pro f, prootic foramen; prsph, parasphenoid; pt, pterygoid; qj, quadratojugal; sph, sphenethmoid; sq, squamosal; vom, vomer; vt, vomerine teeth.

Full-size [DOI: 10.7717/peerj.8642/fig-4](https://doi.org/10.7717/peerj.8642/fig-4)

Maxillary arch (Fig. 4B). Premaxillae paired, anteromedial, longer than high, with a series of 10 teeth, at the anteriormost segments of each maxillary arch, contacting laterally lower part of maxilla. Alary process of premaxilla paired, oriented dorsally, well developed, twice longer than correspondent dentary process. Maxilla paired, longer than premaxillaries, longer than high, higher anteriorly, with a series of approximately 36 teeth, decreasing in size posteriorly. Quadratojugals are positioned posterior to the maxillae and articulates with the angulosphenial.

In ventral view (Fig. 4C), paired vomers, dentigerous and associated with the anterior margins of the sphenethmoid in the palate. The parasphenoid extends posteriorly as a T-shaped ornamented bone.

Lower jaw (Fig. 4B) with paired mentomeckelian bones, dentaries and angulosphenials. Mentomeckelian bone with a very developed fanglike odontoid, oriented dorsally, slightly

smaller than the alary process of premaxilla. A second well developed odontoid occurs in the dentary, posteriorly oriented, no dentition between these two projections. Angulosplenic with a thin row of five odontoids, similar to the correspondent part of maxilla. Odontoids are absent in the juvenile (Fig. 4D).

Tadpole description.— (Fig. 5). Body depressed (wider than high), ovoid in all views, with maximum height and width at the middle third of the body; body length corresponding to approximately 36.1% of total length. Snout uniformly rounded in all views. Eyes dorsally positioned and dorsolaterally directed; eye diameter representing 13.4% of body length. Narial apertures rounded, anterolaterally directed, closer to snout than the eyes; internarial distance representing 26.7% of body width. Spiracle single, sinistral, at the middle third of the body length and below the midline of the body height, directed posterodorsally, with a circular opening, inner wall present as slight ridge, fused to body. Vent tube central, attached to ventral fin, with opening facing the right side.

Oral apparatus (Fig. 5A) in anteroventral position, non-emarginated, surrounded by a single row of small marginal papillae, with an anterior gap on the upper labia. Labial tooth row formula (LTRF) is 2(2)/6, A1 shorter than A2. P1 and P2 of equal size, slightly longer than P3–P6. Jaw sheaths pigmented, with finely serrated edges. Upper jaw sheath arc-shaped and lower jaw sheath U-shaped.

Tail musculature height represents 50% of body height and tapers towards the tip of the tail; myomeres slightly visible in lateral view and clearly visible in dorsal view along the entire length of tail. Dorsal and ventral fins approximately equal in size, dorsal fin begins on body and continues to the tip of the tail, ventral fin begins at the end of the body and continues towards the tip of the tail, which is slightly pointed. The lateral line system is not visible. Measurements are provided in Table S2.

In formalin, the body is translucent, with brown spots distributed on dorsum, ventral and lateral regions. The intestine is visible in all surfaces. The tail is also translucent, with brown spots distributed over the surface.

Variation.— In stage 27, body length corresponding to 36.4% of total length, eye diameter representing 12% of body length, internarial distance representing 27.2% of body width. The LTRF is still not developed with only five posterior tooth rows, the marginal papillae appear in same quantity. Tail musculature height represents 47% of body height and tapers towards the tip of the tail. The maximum tail height is reached in stage 27 (Table S2).

Tadpole comparisons with congeners.— Nine of the 14 species of *Phyllodytes* have described tadpoles (Table S3). Like all their congeners, tadpoles of *P. magnus* have a depressed body (wider than high). Furthermore they have no constriction, a condition similar to *P. acuminatus*, *P. brevirostris*, *P. edelmoi*, *P. melanomystax* and *P. wuchereri*, which contrast to *P. gyrinaethes* which shows anterior and lateral body constrictions and *P. luteolus*, *P. praeceptor* and *P. tuberculosus* which show lateral body constrictions. The LTRF of *P. magnus* is similar to *P. brevirostris* and *P. edelmoi* and differs from the remaining species that show a LTRF 2(2)/3 or 2(2)/4. The most differentiated LTRF appears to occur in *P. praeceptor* (LTRF 1/2) and in *P. gyrinaethes* (LTRF 1(1)/5). The single row of marginal papillae on the oral apparatus of *P. magnus* is similar to *P. gyrinaethes*, *P. luteolus*,

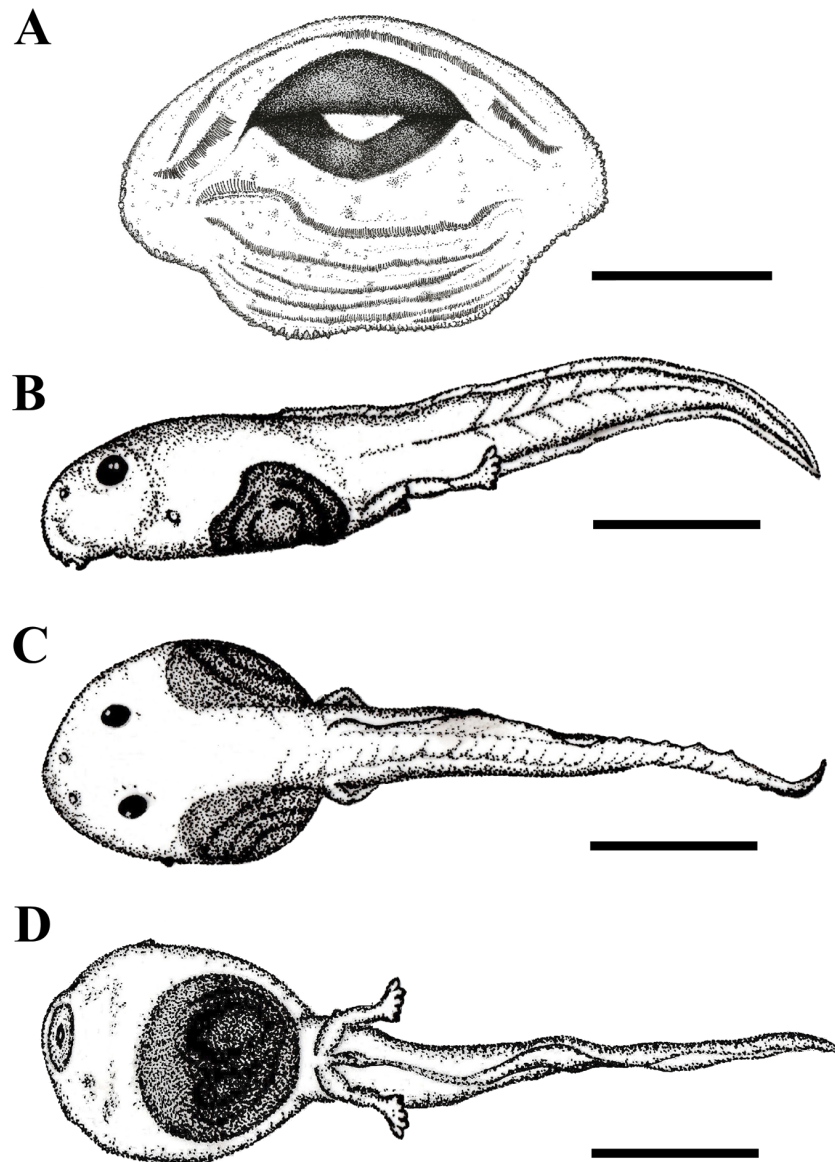


Figure 5 Tadpole of *Phyllodytes magnus* sp. nov. Tadpole at Gosner stage 35 (MZUSP 157525) from Wenceslau Guimarães municipality, State of Bahia, Brazil. (A) oral apparatus, (B) lateral, (C) dorsal and (D) ventral views. Scale bar = one mm (A) and five mm (B, C and D).

Full-size  DOI: [10.7717/peerj.8642/fig-5](https://doi.org/10.7717/peerj.8642/fig-5)

P. melanomystax, *P. tuberculosus* and *P. wuchereri*, and differs from the remaining tadpoles that show at least two posterior rows of marginal papillae.

The dorsal fin of *P. magnus* originating on body is similar to that of *P. brevirostris* and *P. edelmoi* and differs from *P. acuminatus*, *P. gyrinaethes*, *P. praeceptor* and *P. wuchereri* (origin at body-tail junction) and from *P. luteolus*, *P. melanomystax* and *P. tuberculosus* (origin at tail musculature). The ventral fin originating on body is similar to all species of *Phyllodytes* except *P. melanomystax* (at the tail musculature).

Table 1 Quantitative measurements of the advertisement call and of the putative agonistic call (“call type II”) of *Phyllodytes magnus* sp. nov. Data is presented as mean \pm standard deviation (min–max). See text for explanation of measured parameters. –: not measured, see text for explanation. *n* of advertisement calls (for the first three parameters) is 48 and 6 for MZUESC 18264 and MZUESC 18265, respectively. *n* of notes of advertisement calls (for the other parameters) is 91 and 63 for MZUESC 18264 and MZUESC 18265, respectively. For call type II, *n* of calls is eight and *n* of notes is 24.

Acoustic parameters	MZUESC 18264 (holotype)	MZUESC 18265 (paratype)	
		Advertisement call	Call type II
Call duration (s)	5.95 \pm 0.74 (3.85–7.62)	9.60 \pm 1.27(7.54–10.98)	0.92 \pm 0.80 (0.14–2.09)
Call interval (s)	85.61 \pm 55.59 (51.51–430.25)	–	–
Notes per call	9.33 \pm 1.00 (7–11)	27.30 \pm 4.08 (20–31)	3 \pm 2.14 (1–6)
Note duration (s)	0.096 \pm 0.012 (0.055–0.125)	0.086 \pm 0.012 (0.056–0.101)	0.114 \pm 0.05 (0.052–0.241)
Duration 90% (s)	0.044 \pm 0.005 (0.027–0.054)	0.056 \pm 0.012 (0.021–0.068)	0.079 \pm 0.041 (0.028–0.199)
Interval between notes (s)	0.615 \pm 0.146 (0.181–0.960)	0.278 \pm 0.018 (0.233–0.344)	0.281 \pm 0.052 (0.209–0.379)
Note emission rate (note/s)	1.42 \pm 0.40 (0.94–3.61)	2.75 \pm 0.15 (2.29–3.16)	2.54 \pm 0.39 (1.85–3.38)
Note shape	0.77 \pm 0.05 (0.67–0.92)	0.52 \pm 0.13 (0.26–0.81)	0.36 \pm 0.21 (0.01–0.73)
Dominant frequency (kHz)	1.03 \pm 0.04 (0.86–1.29)	0.82 \pm 0.06 (0.78–0.86) /2.15 \pm 0.10 (1.85–2.37)	1.12 \pm 0.53 (0.43–2.15)
Frequency 5% (kHz)	0.88 \pm 0.3 (0.78–0.95)	1.65 \pm 0.40 (0.73–1.89)	0.72 \pm 0.27 (0.47–1.89)
Frequency 95% (kHz)	1.73 \pm 0.19 (1.51–2.76)	2.47 \pm 0.10 (2.20–2.63)	2.02 \pm 0.33 (1.51–2.50)
Bandwidth 90% (kHz)	0.85 \pm 0.19 (0.69–1.81)	0.82 \pm 0.37 (0.52–1.68)	1.30 \pm 0.32 (0.47–1.89)

The spiracle position of *P. magnus*, at midbody, in lower half is similar to those of *P. acuminatus* and *P. wuchereri*, but differs from *P. brevirostris*, *P. luteolus*, *P. melanomystax* and *P. tuberculatus* (at midbody, at midline) and from *P. edelmoi*, *P. praeceptor* and *P. gyrinaethes* (at body’s last third, in lower half). The eye dorsally positioned is similar to *P. acuminatus*, *P. brevirostris*, *P. luteolus*, *P. tuberculatus* and *P. wuchereri*, in contrast to *P. edelmoi*, *P. praeceptor* and *P. melanomystax* (dorso-laterally) and *P. gyrinaethes* (laterally). **Bioacoustics results.**—Quantitative measurements of call parameters and comparisons are summarized in Tables 1 and 2. Like most *Phyllodytes* species, the advertisement call of *P. magnus* is composed by a series of notes of the same type (Fig. 6). Calls are emitted infrequently, separated by up to seven minutes of silence (Table 1). The note begins with a series of well-spaced low-amplitude pulses, which gradually raise in amplitude and emission rate until fusing into the main body of the note (Fig. 6). In the second half of the note, it changes into a sparse-harmonic sound with at least four harmonics and ascending frequency modulation (Fig. 6). The fundamental frequency is also the dominant (Table 1). The amplitude is ordinarily ascendant along the note length, reaching its maximum in the second part, near the note ending (note shape always higher than 0.5, Table 1).

The advertisement call of the paratype MZUESC 18265 has some differences in comparison to the holotype’s call (Table 1). It has more notes per call and higher note emission rate. It also has two discernible parts but, in this case, the first part is much more conspicuous and it has a faster rise of amplitude, which is marked by intense modulations that give a “noisy” (pulsatile) aspect to the waveform and produces many sidebands in the spectrogram (multiples of \sim 0.4 kHz) (Fig. 6). The transition from the first to the second part of the note is well marked by a constriction in the waveform, i.e., an abrupt decay

Table 2 Acoustic parameters from the advertisement calls of *Phyllodytes* species. When available, data is presented as mean ± standard deviation (min–max). When the dominant frequency varies between two or more bands, the values of the different bands are separated by “/”. A sole em dash (—) means data is not available or not applicable. Two adjacent bars (//) indicates an upward modulation from the frequency at the left to the frequency at the right of the bars.

Species	Call duration (s)	Inter-calls interval (s)	Notes per call	Note duration (s)	Inter-notes interval (s)	Dominant frequency (kHz)	1st harmonic (kHz)	Presents Harmonics?	Reference
<i>Phyllodytes magnus</i> sp. nov.	6.36 ± 1.41 (3.85–10.98)	85.61 ± 55.59(51.51–430.25)	11.33 ± 5.92 (7–31)	0.092 ± 0.013 (0.055–0.125)	0.470 ± 0.200(0.181–0.960)	1.47 ± 0.56(0.78–2.37)	0.51 ± 0.05 (0.39–0.60) // 1.08 ± 0.04 (0.95–1.16)	Yes	This paper
<i>P. amadoi</i>	3.41 ± 0.28(2.99–4.11)	53.4 ± 8.5(41–68)	14.5 ± 1(13–17)	0.043 ± 0.021(0.008–0.119)	0.204 ± 0.02(0.137–0.285)	3.76 ± 0.40(2.41–4.31)	—	No	Vörös, Dias & Solé (2017)
<i>P. acuminatus</i>	—	18.99 ± 11.18 (6.03–53.4)	1–4	0.10 ± 0.03(0.03–0.17)	0.35 ± 0.05 (0.27–0.47)	2.14 ± 0.09 (2.07–2.33) / 4.28 ± 0.15 (4.05–4.57)	2.14 ± 0.09 (2.07–2.33)	Yes	Campos et al. (2014)
<i>P. edelmoi</i>	5.2 ± 0.44 (4.28–5.73)	48.27 ± 8.33 (38.11–64.83)	26.46 ± 2.3 (22–29)	0.1 ± 0.003 (0.04–0.16)	—	2.84 ± 0.16(1.49–3.32)	—	No	Lima, Lingnau & Skuk (2008)
<i>P. gyrinaethes</i>	1.7 ± 0.3(1.3–2.3)	52.4 ± 25.7 (21.2–88.7)	4.9 ± 0.6(4–6)	0.04 ± 0.01 (0.02–0.07)	0.4 ± 0.03(0.3–0.5)	2.75 ± 0.16(2.53–3.09)	—	No	Roberto & Ávila (2013)
<i>P. kautskyi</i>	3.55 ± 0.19	46.66 ± 11.45	21	0.085 ± 0.012	0.066–0.120	1.37(0.87 // 1.81)	1.37(0.87 // 1.81)	Yes	Simon & Gasparini (2003)
<i>P. luteolus</i>	5	—	8–15	0.125	—	2–6*	—	No	Weygoldt (1981)
<i>P. megatympaum</i>	5.91 ± 4.56 (3.2–23.63)	30.9 ± 10.31 (6.96–47.58)	13.37 ± 2.56 (10–19)	0.092 ± 0.08 (0.009–0.245)	0.305 ± 0.1(0.1–0.62)	3.98 ± 0.136 (3.56–4.12)	1.98	Yes	Marciano-Jr, Lantyer-Silva & Solé (2017)
<i>P. melanomystax</i>	0.07 ± 0.04	28.81 ± 12.48 (11.18–54.29)	1	0.07 ± 0.04	28.81 ± 12.48 (11.18–54.29)	1.39 ± 0.05 / 3.11 ± 0.25	1.39 ± 0.05	Yes	Nunes, Santiago & Juncá (2007)
<i>P. praeceptor</i>	5.34 ± 1.53(3.02–9.41)	48.5 ± 21.2(29.5–99.2)	8.39 ± 1.55(6–12)	0.295 ± 0.075(0.141–0.538)	0.389 ± 0.102(0.236–1.057)	3.05 ± 0.12(2.93–3.27)	—	No	Orrico, Dias & Marciano-Jr (2018)
<i>P. tuberculatus</i>	6.72 ± 1.73 (4.65–9.35)	—	18.60 ± 3.36 (14–23)	0.167 ± 0.047 (0.068–0.246)	0.214 ± 0.048 (0.067–0.357)	2.46 ± 0.45 (1.68–3.27)	—	No	Juncá et al. (2012)
<i>P. wuchereri</i>	2.8–6.8	134 ± 10 (120–143)	10–21	0.05–0.32	0.09–0.21	1.12–1.46 / 2.67–3.53	—	No	Cruz, Marciano & Napoli (2014) and Magalhães, Juncá & Garda (2015)

Notes.

*These values, separated by en dash, are not minimum and maximum in the statistical sense, instead they represent approximately the minimum and maximum of a frequency bandwidth.

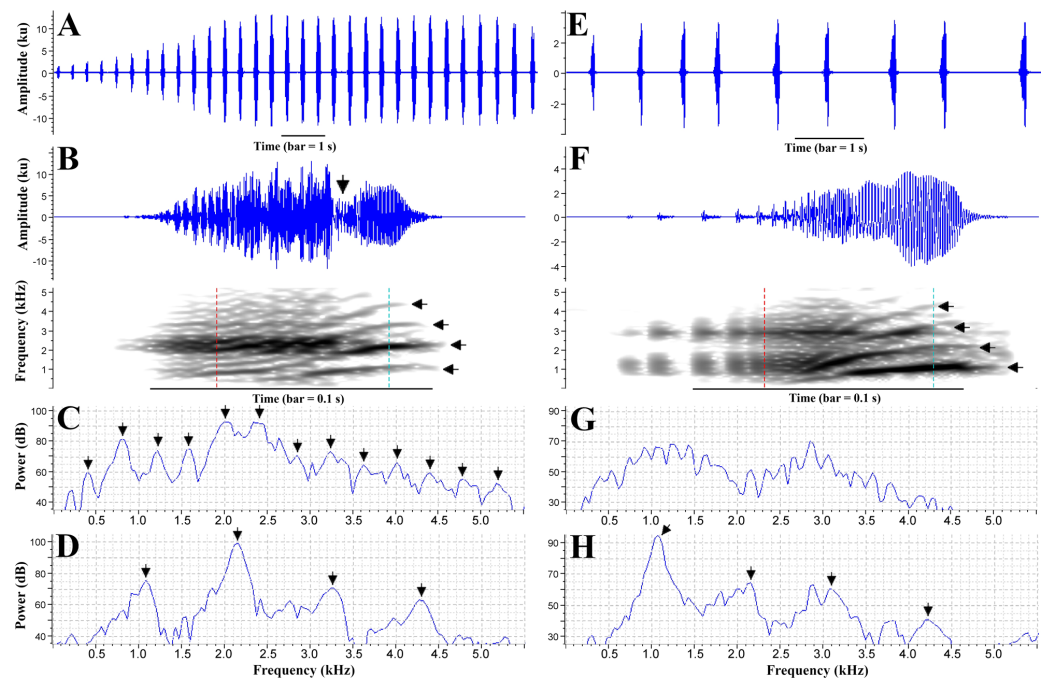


Figure 6 Advertisement call of *Phyllodytes magnus* sp. nov. Graphic representations of the advertisement call of the paratype MZUESC 18265 (A–D) and of the holotype MZUESC 18264 (E–H) of *Phyllodytes magnus* sp. nov. A and E: waveform of an entire call. B and F: waveform and spectrogram of one note; vertical arrow in waveform in B indicates the constriction of the waveform (see text for explanation); horizontal arrows in the spectrogram indicate the harmonics; vertical dashed lines in the spectrograms indicate the position of the spectrogram slices. C and G: spectrogram slice of the first part of the note (indicated by the left vertical line) in B and F, respectively; arrows in C indicate the sidebands, multiples of ~ 0.4 kHz (see text for explanation). D and H: spectrogram slice of the second part of the note (indicated by the right vertical line) in B and F, respectively; arrows indicate the harmonics, multiples of ~ 1.07 kHz (see text for explanation). Spectrographic views settings: window type: Hann, window size: 512 samples, 3 dB filter bandwidth: 124 Hz, time grid overlap: 90%, time grid size: 51 samples, frequency grid DFT size: 512 samples, frequency grid spacing: 86.1 Hz. Call voucher –FNJV 40997 (holotype) and FNJV 41382–41384 (MZUESC 18265).

Full-size [DOI: 10.7717/peerj.8642/fig-6](https://doi.org/10.7717/peerj.8642/fig-6)

followed by a subsequent rise of amplitude (Fig. 6). The note shape is way more variable than that of the holotype (Table 1) because the maximum amplitude is reached sometimes near the beginning of note and sometimes near its ending.

We believe the differences between the calls of the two recorded individuals are due to their different levels of motivation or due to geographic variation. Further studies should address the variation in advertisement calls of this species.

A second type of call was emitted exclusively in response to our imitations, suggesting an agonistic function. This call is composed by a single note or a series of up to six notes with decreasing duration. The first notes (“A notes”) have conspicuous secondary amplitude modulation, giving a “multipulsed” fashion to the waveform with up to five amplitude peaks (“pulses”) (Fig. S3). The spectrogram of this type of note has harmonics and fast A-shaped frequency modulations (Fig. S3). The last notes of the series (“B notes”) resemble the notes of the advertisement call. This type of call was emitted with much lower

amplitude, only about one tenth of the maximum amplitude of the advertisement call. The duration of note of call type II is slightly longer than the duration of advertisement call note, but regarding the dominant frequency there is no great difference between the two types of call (Table 1).

Bioacoustic comparisons with congeners.— The advertisement call of *Phyllodytes magnus* is unique in the genus by having composite notes with two components of approximately same duration: the first, pulsed/pulsatile, and the second, harmonic (Table 2). Though *P. melanomystax* also presents composite notes, its harmonic component is much longer than the noisy (pulsatile) component, which is present both in the beginning and in the end of the note (Fig. S4). The other species calls have either exclusively pulsed/pulsatile (*P. amadoi*, *P. edelmoi*, *P. gyrinaethes*, *P. luteolus*, *P. tuberculosus*, *P. praeceptor* and *P. wuchereri*) or harmonic (*P. acuminatus*, *P. kautskyi*, *P. megatympanum*) notes.

Furthermore, the dominant frequency in *Phyllodytes magnus* (0.78–2.37 kHz) is lower than in *P. amadoi*, *P. gyrinaethes*, *P. megatympanum* and *P. praeceptor* (combined dominant frequencies: 2.41–4.31 kHz), as well as the frequency of the first harmonic in *P. magnus* (0.39–1.16 kHz) is lower than in *P. acuminatus*, *P. megatympanum* and *P. melanomystax* (combined first harmonic frequencies: 1.39–2.33 kHz). The number of notes per call in *P. magnus* (7–31 notes) is higher than in *P. acuminatus* (1–4 notes), *P. gyrinaethes* (4–6 notes) and *P. melanomystax* (single-note call). The advertisement call of *Phyllodytes magnus* can be distinguished from *P. kautskyi* by lacking a downward frequency modulation at the end of the note (marked in *P. kautskyi* - see Simon & Gasparini, 2003) and by a longer interval between the notes (*P. magnus* = 0.181–0.960 s versus *P. kautskyi* = 0.066–0.120 s).

Molecular results.— Our results recovered *Phyllodytes* as a well-supported monophyletic group (Fig. 7), in a polytomy together with *Tepuihyla*, *Osteopilus* and *Osteocephalus* + *Dryaderces*. The relationships of the main clades recovered within Lophyohylini received low support, as well as within *Phyllodytes*. The new species was recovered as sister to other analyzed species of *Phyllodytes* (Fig. 7). Values of genetic distance between *Phyllodytes magnus* and the other analyzed species of the genus range between 6.4 to 10.2% being lowest compared to *P. luteolus* (Table S4).

Cytogenetic results.— We analyzed 35 somatic metaphases and defined the diploid number of $2n = 22$ chromosomes and $NF = 44$ (Fig. 8A). Chromosome pairs 1, 7, 8, 9, 10 and 11 are metacentric, pairs 2, 3, 5 and 6 submetacentric and pair 4 subtelocentric. C banding identified a small amount of constitutive heterochromatin, as conspicuous blocks positioned pericentrically in all chromosomes. The NORs are euchromatic (Fig. 8B). The impregnation with silver nitrate showed single NORs placed terminally in the long arms of pair 2. The number and position of NORs sites were confirmed after FISH with 18S rDNA probe (Fig. 8C, Fig. 8D).

Geographic Distribution and Natural history.— *Phyllodytes magnus* is known from three localities from the Atlantic Rainforest of Bahia (Fig. S5). Calls of this species have also been heard in the municipalities of Almadina, Ilhéus, Igrapiúna and Camacan, state of Bahia, but as no vouchers or recordings were obtained, these records need to be confirmed.

Although one specimen of *Phyllodytes magnus* was in a ground bromeliad, most calling males were in canopy bromeliads. At Parque Estadual da Serra do Conduru, *Phyllodytes*

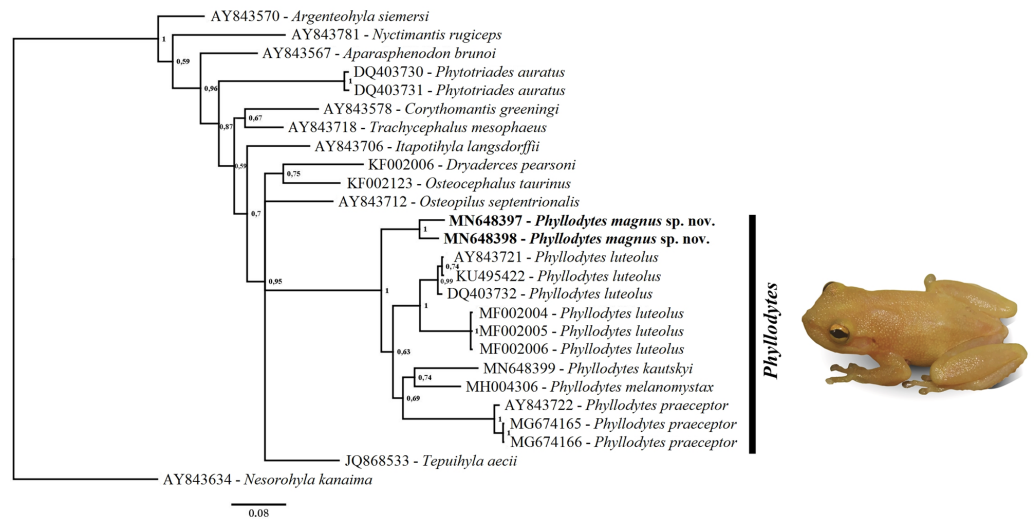


Figure 7 Phylogenetic relationship of genus *Phyllodytes* through 16S mitochondrial rRNA fragment gene (791 bp). Bayesian posterior probabilities values are indicated close to the branches.

Full-size [DOI: 10.7717/peerj.8642/fig-7](https://doi.org/10.7717/peerj.8642/fig-7)

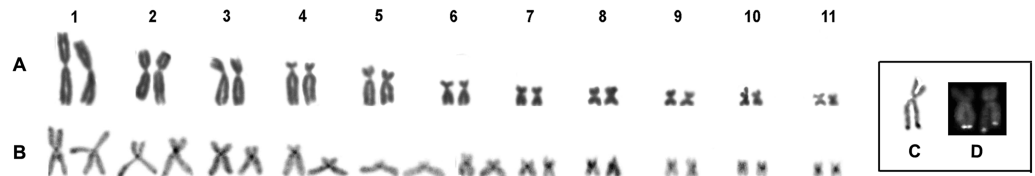


Figure 8 Karyotype of *Phyllodytes magnus* sp. nov. Giemsa staining (A) and C-banding (B). Highlighted are the NOR-bearing chromosomes after silver nitrate staining (C) and FISH with 18S rDNA probe (D).

Full-size [DOI: 10.7717/peerj.8642/fig-8](https://doi.org/10.7717/peerj.8642/fig-8)

magnus is syntopic with four congeners (*P. maculosus*, *P. megalotympanum*, *P. melanomystax* and *P. praeceptor*), although apparently less abundant than its relatives. In an area of 52 ha we heard only five males in a one-night search. All were calling from epiphytic giant bromeliads of the genus *Hohenbergia* with diameter superior to 1.50 m and at heights between 3.10 m and 11.30 m ($x = 7.72 \text{ m} \pm 3.56 \text{ m}$). We found a male of *Phyllodytes melanomystax* in the same bromeliad where we collected the paratype MZUESC 18265, though in a different axil.

DISCUSSION

Phyllodytes magnus can be readily distinguished from their congeners by morphological (large size and immaculate dorsum), acoustical (advertisement call with 7 to 31 notes; amplitude modulated notes with the first part pulsed/pulsatile and the second part sparse-harmonic) and molecular characteristics (>6% genetic distance from all analyzed congeners).

We remark for the first time the presence of composite notes (i.e., a note composed by a harmonic part plus a pulsed/pulsatile part) in the advertisement call of a *Phyllodytes* species. When comparing the calls of congeners we found that this feature occurs in *Phyllodytes melanomystax* as well. This can be observed, in the waveform, as an intense amplitude modulated (noisy) section and, in the spectrogram, as a dense and broad range of sidebands, both in the beginning and in the end of the note, while the midnote is comprised by a less noisy waveform and harmonics in the spectrogram (Fig. S4). We believe that what Nunes, Santiago & Juncá (2007) interpreted as being artifacts in the call of *P. melanomystax* may actually represent these natural components. We recommend that further call descriptions should pay attention to this feature as it seems to be an important character and can be more widespread in the genus, as well as in other frogs (e.g., *Hyla gratiosa*, see Gerhardt, 1981).

Although there are proposals to allocate *Phyllodytes* species into groups based on color pattern (Peixoto, Caramaschi & Freire, 2003; Caramaschi, Peixoto & Rodrigues, 2004) or bioacoustic characteristics (Roberto & Ávila, 2013), it has only been possible to test these proposals very recently within a more comprehensive phylogenetic context and none of them have been recovered as monophyletic (Blotto et al., 2020). Another question that hangs on *Phyllodytes* is its relationship with *Phytotriades*. Most of the studies did not recover this genus as sister taxon (e.g., Jowers, Downie & Cohen, 2008; Wiens et al., 2010; Pyron & Wiens, 2011; Pyron, 2014; Ron et al., 2016; Jetz & Pyron, 2018) although other authors obtained this result (Moen & Wiens, 2009; Duellman, Marion & Hedges, 2016). Even when we increase the number of analyzed species of *Phyllodytes* (previously there were only two species of this genus with sequences available for analysis) we did not recover these genera as close relatives. The same result was obtained in a phylogenetic study contemplating a larger sampling of mitochondrial and nuclear genes from more than 96% of the species of the Lophyohylini tribe and all recognized *Phyllodytes* species, including *P. magnus* as *P. sp. 2* (Blotto et al., 2020).

Phyllodytes magnus presents $2n = 22$ chromosomes and single NORs placed in the terminal region of the long arms of pair 2, the same condition described to *P. luteolus* and *P. edelmoi* (Gruber, Haddad & Kasahara, 2012) the only two species cytogenetically studied. However, *P. magnus* has a different macrochromosome arrangement. The most frequent chromosome number in Hylidae is $2n = 24$, however, variations of this diploid number are not rare for this family (Baldissera Jr, Oliveira & Kasahara, 1993; Catroli & Kasahara, 2009). Gruber, Haddad & Kasahara (2012) proposed that the diploid number reduction observed in *Phyllodytes* should be considered as a synapomorphy for the genus, a result of a chromosomal fusion involving the nucleolar chromosomes. Our data confirmed this proposal and the few differences in the macro - (pairs 4 and 6) and microchromosome constitution (C-banding pattern) between these species are probably results of non-robertsonian rearrangements. Too few is known about cytogenetic of species of *Phyllodytes*. This lack of knowledge does not allow a more robust discussion about the patterns of chromosomal evolution in the genus.

CONCLUSIONS

Almost 60% (nine species) of the known diversity of *Phyllodytes* can be found in the Atlantic Forest of southern Bahia, the region with the highest concentration of representatives of this genus. Over half of these species are endemic to the state: *P. wuchereri*, *P. praeceptor*, *P. megatympanum*, *P. amadoi* and *P. magnus*, the latter three are known from a few localities or only from the type locality (Cruz, Marciano & Napoli, 2014; Marciano-Jr, Lantyer-Silva & Solé, 2017; Vörös, Dias & Solé, 2017; this study). The high diversity of *Phyllodytes* in this part of the central corridor of the Atlantic Forest (Carnaval et al., 2009) is not unique. Other genera like *Adelophryne* (Fouquet et al., 2012; Lourenço-de Moraes et al., 2018), *Adenomera* (Fouquet et al., 2014), *Gastrotheca* (Teixeira-Jr et al., 2012) or the gymnophthalmid lizard genus *Leposoma* (Rodrigues et al., 2013), to cite a few, have their highest species diversity in this part of the biome. The high diversity of *Phyllodytes* and endemism brings support to this pattern and highlights the evolutionary importance of this area. Furthermore, together with the scarce available biological information and habitat specificity (bromeliads), it makes the Atlantic Forest of the state of Bahia a priority area for research and conservation of *Phyllodytes*.

ACKNOWLEDGEMENTS

We thank Carlos Augusto Souza-Costa and Joedison dos Santos Rocha for their support in the field and Ana Paula Barbosa for her support in lab work. We are also grateful to the “Grupo Ambientalista da Bahia” - GAMBA for lodging and logistic support in Serra da Jibóia. We also thank Rogério Miranda Ribeiro and the staff from SEMA for the permits to work at Estação Ecológica Wenceslau Guimarães (2011-020194). We thank Rodrigo Barbosa Ferreira, Luciana Fusinato and one anonymous referee for their careful reading of the manuscript and suggestions.

ADDITIONAL INFORMATION AND DECLARATIONS

Funding

Scholarships were provided by the Coordenação de Aperfeiçoamento de Pessoal de Nível Superior and Conselho Nacional de Desenvolvimento Científico e Tecnológico (CNPq—Project: 406899/2017-7, process: 167387/2017-0 and 155198/2018-1) to Iuri Ribeiro Dias. Scholarships were provided by Fundação de Amparo à Pesquisa do Estado da Bahia (FAPESB; No BOL1767/2013) and by CAPES (masters degree scholarship between 2016–2017) to Gabriel Novaes e Fagundes. Mirco Solé was funded by a “Bolsa de Produtividade em Pesquisa” (CNPq–304999/2015–6), a “Universal” project (CNPq–449930/2014–9) and a “PROTAX” project (CNPq–440615/2015–1). Fundação O Boticário de Proteção à Natureza (0991_20132) funded this study. Miguel Trefaut Rodrigues received funding from the Fundação de Amparo à Pesquisa do Estado de São Paulo (project 2011/50146-6) and CNPq. Antonio Mollo Neto received funding from Fundação de Amparo à Pesquisa do Estado de São Paulo (project 2017/15025-0). There was no additional external funding

received for this study. The funders had no role in study design, data collection and analysis, decision to publish, or preparation of the manuscript.

Grant Disclosures

The following grant information was disclosed by the authors:

Coordenação de Aperfeiçoamento de Pessoal de Nível Superior and Conselho Nacional de Desenvolvimento Científico e Tecnológico (CNPq–Project: 406899/2017-7, Process: 167387/2017-0 and 155198/2018-1).

Fundação de Amparo à Pesquisa do Estado da Bahia: No BOL1767/2013.

CAPES (masters degree scholarship between 2016–2017).

Bolsa de Produtividade em Pesquisa” (CNPq–304999/2015–6).

A “Universal” project (CNPq–449930/2014–9).

A “PROTAX” project (CNPq–440615/2015–1).

Fundação O Boticário de Proteção à Natureza (0991_20132).

Fundação de Amparo à Pesquisa do Estado de São Paulo: project 2011/50146-6, project 2017/15025-0.

Competing Interests

The authors declare there are no competing interests.

Author Contributions

- Iuri R. Dias, Gabriel Novaes-e-Fagundes, Antonio Mollo Neto and Caroline Garcia conceived and designed the experiments, performed the experiments, analyzed the data, prepared figures and/or tables, authored or reviewed drafts of the paper, and approved the final draft.
- Juliana Zina, Renato Sousa Recoder, Francisco Dal Vechio, Miguel Trefaut Rodrigues and Mirco Solé conceived and designed the experiments, authored or reviewed drafts of the paper, and approved the final draft.

Animal Ethics

The following information was supplied relating to ethical approvals (i.e., approving body and any reference numbers):

This research was approved by the ethics committee on the use of animals (CEUA-UESC 002/12). Specimens collected for this manuscript were obtained under IBAMA #12920-1 and ICMBIO #13708-1 and #35068 permits.

DNA Deposition

The following information was supplied regarding the deposition of DNA sequences:

New sequences of *Phyllodytes magnus* sp. nov. (MZUESC 18264 and 18265) and *P. kautskyi* (MBML 8818) are available at GenBank: [MN648397](#) to [MN648399](#).

Raw sequence data is available in the [Supplemental File](#).

Data Availability

The following information was supplied regarding data availability:

All recordings are available at the Fonoteca Neotropical Jacques Vielliard (<https://www2.ib.unicamp.br/fnjv/>): FNJV 40997, 41382-41384 and in the [Supplemental Files](#). Additional data is available at Morphosource: https://www.morphosource.org/Detail/MediaDetail/Show/media_id/47746.

New Species Registration

The following information was supplied regarding the registration of a newly described species:

Publication LSID: urn:lsid:zoobank.org:pub:FD2CACD2-F59F-4B75-947D-B576701424D9

Phyllodytes magnus LSID: urn:lsid:zoobank.org:act:D8DF9024-57C1-413B-9D05-B0CF05B7929C.

Supplemental Information

Supplemental information for this article can be found online at <http://dx.doi.org/10.7717/peerj.8642#supplemental-information>.

REFERENCES

- Altig R, McDiarmid RW. 1999.** Body plan: development and morphology. In: McDiarmid RW, Altig R, eds. *Tadpoles: the biology of anuran larvae*. Chicago: The University of Chicago Press, 24–51.
- Baldissera Jr FA, Oliveira PSL, Kasahara S. 1993.** Cytogenetics of four Brazilian *Hyla* species (Amphibia –Anura) and description of a case with a supernumerary chromosome. *Brazilian Journal of Genetics* **16**:335–345.
- Beeman K. 1998.** Digital signal analysis, editing, and synthesis. In: Hopp SL, Owren MJ, Evans CS, eds. *Animal acoustic communication: sound analysis and research methods*. Berlin: Springer Verlag, 59–103.
- Blotto BL, Lyra ML, Cardoso MCS, Rodrigues MT, Dias IR, Marciano-Jr E, Vechio FD, Orrico VGD, Brandão RA, Assis CL, Lantyer-Silva ASF, Rutherford MG, Gagliardi-Urrutia G, Solé M, Baldo D, Nunes I, Cajade R, Torres A, Grant T, Jungfer KH, Silva HR, Haddad CFB, Faivovich J. 2020.** The phylogeny of the Casque-headed Treefrogs (Hylidae: Hylinae: Lophohylini). *Cladistics* Epub ahead of print 2020 27 March DOI [10.1111/cla.12409](https://doi.org/10.1111/cla.12409).
- Bokermann WCA. 1966.** O gênero *Phyllodytes* Wagler, 1830 (Anura, Hylidae). *Anais da Academia Brasileira de Ciências* **38**:335–344.
- Campos TF, Lima MG, Nascimento AC, Santos EM. 2014.** Larval morphology and advertisement call of *Phyllodytes acuminatus* Bokermann, 1966 (Anura: Hylidae) from northeastern Brazil. *Zootaxa* **3779**:93–100 DOI [10.11646/zootaxa.3779.1.10](https://doi.org/10.11646/zootaxa.3779.1.10).
- Caramaschi U, Peixoto OL, Rodrigues MT. 2004.** Revalidation and redescription of *Phyllodytes wuchereri* (Peters, 1873) (Amphibia, Anura, Hylidae). *Arquivos do Museu Nacional, Nova Série, Zoologia* **62**:185–191.

- Carnaval AC, Hickerson MJ, Haddad CFB, Rodrigues MT, Moritz C. 2009. Stability predicts genetic diversity in the Brazilian Atlantic Forest hotspot. *Science* **323**:785–789 DOI [10.1126/science.1166955](https://doi.org/10.1126/science.1166955).
- Catrolí GF, Kasahara S. 2009. Cytogenetic data on species of the family Hylidae (Amphibia, Anura): results and perspectives. *Publicatio UEPG: Ciências Biológicas e da Saúde* **15**:67–86.
- Charif RA, Waack AM, Strickman LM. 2010. *Raven Pro 1.4 User's Manual*. Ithaca: Cornell Lab of Ornithology.
- Cruz CAG, Feio RN, Cardoso MCS. 2006. Description of a new species of *Phyllodytes* Wagler, 1830 (Amphibia, Anura, Hylidae) from the Atlantic Rain Forest of the State of Minas Gerais and Bahia. *Arquivos do Museu Nacional do Rio de Janeiro* **64**:321–324.
- Cruz D, Marciano JRE, Napoli MF. 2014. Advertisement and courtship calls of *Phyllodytes wuchereri* (Peters, 1873) (Anura: Hylidae). *Zootaxa* **3774**:7–100.
- Cunha MS, Napoli MF. 2016. Calling site selection by the bromeliad-dwelling treefrog *Phyllodytes melanomystax* (Amphibia: Anura: Hylidae) in a coastal sand dune habitat. *Studies on Neotropical Fauna and Environment* **51**:144–151.
- Darriba D, Taboada GL, Doallo R, Posada D. 2012. jModelTest 2: more models, new heuristics and parallel computing. *Nature Methods* **98**:772.
- Darst CR, Cannatella DC. 2004. Novel relationships among hyloid frogs inferred from 12S and 16S mitochondrial DNA sequences. *Molecular Phylogenetics and Evolution* **31**:462–475 DOI [10.1016/j.ympev.2003.09.003](https://doi.org/10.1016/j.ympev.2003.09.003).
- Dias IR, Medeiros T, Nova MV, Solé M. 2014. Amphibians of Serra Bonita, southern Bahia: a new hotspot within Brazil's Atlantic Forest hotspot. *ZooKeys* **449**:105–130 DOI [10.3897/zookeys.449.7494](https://doi.org/10.3897/zookeys.449.7494).
- Dias IR, Mira-Mendes CV, Solé M. 2014. Rapid inventory of herpetofauna at the APA (environmental protection area) of the Lagoa Encantada and Rio Almada, Southern Bahia, Brazil. *Herpetology Notes* **7**:627–637.
- Duellman WE, Marion AB, Hedges SB. 2016. Phylogenetics, classification, and biogeography of the treefrogs (Amphibia: Anura: Arboranae). *Zootaxa* **4104**:1–109 DOI [10.11646/zootaxa.4104.1.1](https://doi.org/10.11646/zootaxa.4104.1.1).
- Duellmann WE, Trueb L. 1986. *Biology of amphibians*. New York: McGraw-Hill.
- Faivovich J, Haddad CFB, Garcia PCA, Frost DR, Campbell JA, Wheeler WC. 2005. Systematic review of the frog family Hylidae, with special reference to Hylinae: phylogenetic analysis and taxonomic revision. *Bulletin of the American Museum of Natural History* **294**:1–240 DOI [10.1206/0003-0090\(2005\)294\[0001:SROTFF\]2.0.CO;2](https://doi.org/10.1206/0003-0090(2005)294[0001:SROTFF]2.0.CO;2).
- Ferreira RB, Schneider JA, Teixeira RL. 2012. Diet, fecundity, and use of bromeliads by *Phyllodytes luteolus* (Anura: Hylidae) in Southeastern Brazil. *Journal of Herpetology* **46**:19–24 DOI [10.1670/09-040](https://doi.org/10.1670/09-040).
- Fouquet A, Cassini CS, Haddad CFB, Pech N, Rodrigues MT. 2014. Species delimitation, patterns of diversification and historical biogeography of the Neotropical frog genus *Adenomera* (Anura, Leptodactylidae). *Journal of Biogeography* **41**:855–870 DOI [10.1111/jbi.12250](https://doi.org/10.1111/jbi.12250).

- Fouquet A, Loebmann D, Castroviejo-Fisher S, Padial JM, Orrico VGD, Lyra ML, Roberto IJ, Kok PJR, Haddad CFB, Rodrigues MT. 2012.** From Amazonia to the Atlantic forest: Molecular phylogeny of Phyzelaphryninae frogs reveals unexpected diversity and a striking biogeographic pattern emphasizing conservation challenges. *Molecular Phylogenetics and Evolution* **65**:547–561 DOI [10.1016/j.ympev.2012.07.012](https://doi.org/10.1016/j.ympev.2012.07.012).
- Freitas MA. 2015.** *Herpetofauna no Nordeste Brasileiro*. Rio de Janeiro, Technical Books Editora.
- Freitas MA, Abegg AD, Dias IR, Moraes EPF. 2018.** Herpetofauna from Serra da Jibóia, an Atlantic Rainforest remnant in the state of Bahia, northeastern Brazil. *Herpetology Notes* **11**:59–72.
- Frost DR. 2019.** Amphibian species of the world: an online reference. Electronic Database. Version 6.0. New York, USA: American Museum of Natural History. Available at <http://research.amnh.org/herpetology/amphibia/index.html> (accessed on 20 August 2019).
- Gerhardt HC. 1981.** Mating call recognition in the Barking Treefrog (*Hyla gratiosa*): responses to synthetic calls and comparisons with the Green Treefrog (*Hyla cinerea*). *Journal of Comparative Physiology* **144**:17–25 DOI [10.1007/BF00612793](https://doi.org/10.1007/BF00612793).
- Gosner KL. 1960.** A simplified table for staging anuran embryos and larvae with notes on identification. *Herpetologica* **16**:183–190.
- Gruber SL, Haddad CF, Kasahara S. 2012.** Karyotype analysis of seven species of the tribe Lophiohylini (Hylinae, Hylidae, Anura), with conventional and molecular cytogenetic techniques. *Comparative Cytogenetics* **6**:409–423 DOI [10.3897/compcytogen.v6i4.3945](https://doi.org/10.3897/compcytogen.v6i4.3945).
- Hatanaka T, Galetti PM. 2004.** Mapping of the 18S and 5S ribosomal RNA genes in the fish *Prochilodus argenteus* Agassiz, 1829 (Characiformes, Prochilodontidae). *Genetica* **122**:239–244 DOI [10.1007/s10709-004-2039-y](https://doi.org/10.1007/s10709-004-2039-y).
- Heyer WR, Rand AS, Cruz CAG, Peixoto OL, Nelson CE. 1990.** Frogs of Boracéia. *Arquivos de Zoologia* **31**:231–410.
- Howell WM, Black DA. 1980.** Controlled silver staining of nucleolar organizer regions with a protective colloidal developer; a 1-step method. *Experientia* **36**:1014–1015 DOI [10.1007/BF01953855](https://doi.org/10.1007/BF01953855).
- Huelsenbeck JP, Ronquist F. 2001.** MrBayes: bayesian inference of phylogenetic trees. *Bioinformatics* **17**:754–755 DOI [10.1093/bioinformatics/17.8.754](https://doi.org/10.1093/bioinformatics/17.8.754).
- Jetz W, Pyron RA. 2018.** The interplay of past diversification and evolutionary isolation with present imperilment across the amphibian tree of life. *Nature Ecology and Evolution* **2**:850–858 DOI [10.1038/s41559-018-0515-5](https://doi.org/10.1038/s41559-018-0515-5).
- Jowers MJ, Downie JR, Cohen BL. 2008.** The Golden Tree Frog of Trinidad, *Phyllodytes auratus* (Anura: Hylidae): systematic and conservation status. *Studies on Neotropical Fauna and Environment* **43**:181–188 DOI [10.1080/01650520801965490](https://doi.org/10.1080/01650520801965490).
- Juncá FA, Napoli MF, Cedraz J, Nunes I. 2012.** Acoustic characteristics of the advertisement and territorial calls of *Phyllodytes tuberculatus* Bokermann, 1966 (Amphibia: Anura: Hylidae). *Zootaxa* **3506**:87–88.

- Katoh K, Toh H. 2008.** Recent developments in the MAFFT multiple sequence alignment program. *Briefings in Bioinformatics* **9**:276–285 DOI [10.1093/bib/bbn015](https://doi.org/10.1093/bib/bbn015).
- King M, Rofe R. 1976.** Karyotype variation in the Australian gekko *Phyllodactylus marmoratus* (Gray) (Gekkonidae: Reptilia). *Chromosoma* **54**:75–87 DOI [10.1007/BF00331835](https://doi.org/10.1007/BF00331835).
- Köhler J, Jansen M, Rodríguez A, Kok PJR, Toledo LF, Emmrich M, Glaw F, Haddad CFB, Rödel MO, Vences M. 2017.** The use of bioacoustics in anuran taxonomy: theory, terminology, methods and recommendations for best practice. *Zootaxa* **4251**:1–124 DOI [10.11646/zootaxa.4251.1.1](https://doi.org/10.11646/zootaxa.4251.1.1).
- Kok PJR, Kalamandeen M. 2008.** Introduction to the taxonomy of the amphibians of Kaieteur national Park, Guyana. *Abc Taxa* **5**:1–278.
- Levan A, Fredga K, Sandberg AA. 1964.** Nomenclature for centromeric position on chromosomes. *Hereditas* **52**:201–220.
- Lewis CT, Short C. 1891.** *A New Latin Dictionary, Founded on Andrews' edition of Freund's Latin dictionary. Revised, enlarged, and in great part rewritten.* New York, Oxford: Clarendon Press.
- Lima MG, Lingnau R, Skuk GO. 2008.** The Advertisement call of *Phyllodytes edelmoi* (Anura, Hylidae). *South American Journal of Herpetology* **3**:118–121 DOI [10.2994/1808-9798\(2008\)3\[118:TACOPE\]2.0.CO;2](https://doi.org/10.2994/1808-9798(2008)3[118:TACOPE]2.0.CO;2).
- Littlejohn MJ. 2001.** Patterns of differentiation in temporal properties of acoustic signals of anurans. In: Ryan M, ed. *Anuran communication.* Washington and London: Smithsonian Institution Press, 102–120.
- Lourenço-de Moraes R, Dias IR, Mira-Mendes CV, Oliveira RM, Barth A, Ruas DS, Vences M, Solé M, Bastos RP. 2018.** Diversity of miniaturized frogs of the genus *Adelophryne* (Anura: Eleutherodactylidae): A new species from the Atlantic Forest of northeast Brazil. *PLOS ONE* **139**:e0201781.
- Magalhães FDM, Juncá FA, Garda AA. 2015.** Tadpole and vocalisations of *Phyllodytes wuchereri* (Anura: Hylidae) from Bahia, Brazil. *Salamandra* **51**:83–90.
- Marciano-Jr E, Lantyer-Silva AS, Solé M. 2017.** A new species of *Phyllodytes* Wagler, 1830 (Anura, Hylidae) from the Atlantic Forest of southern Bahia, Brazil. *Zootaxa* **4238**:135–142 DOI [10.11646/zootaxa.4238.1.11](https://doi.org/10.11646/zootaxa.4238.1.11).
- Miller MA, Pfeiffer W, Schwartz T. 2010.** Creating the CIPRES Science Gateway for inference of large phylogenetic trees. In: *Proceedings of the Gateway Computing Environments Workshop (GCE).* New Orleans, 1–8.
- Mira-Mendes CB, Ruas DS, Oliveira RM, Castro IM, Dias IR, Baumgarten JE, Juncá FA, Solé M. 2018.** Amphibians of the Reserva Ecológica Michelin: a high diversity site in the lowland Atlantic Forest of southern Bahia, Brazil. *ZooKeys* **753**:1–21 DOI [10.3897/zookeys.753.21438](https://doi.org/10.3897/zookeys.753.21438).
- Moen DS, Wiens JJ. 2009.** Phylogenetic evidence for competitively driven divergence: body-size evolution in caribbean treefrogs (Hylidae: *Osteopilus*). *Evolution* **63**:195–214 DOI [10.1111/j.1558-5646.2008.00538.x](https://doi.org/10.1111/j.1558-5646.2008.00538.x).

- Nunes I, Santiago RS, Juncá FA. 2007.** Advertisement calls of four hylid frogs from the state of Bahia, northeastern Brazil (Amphibia, Anura, Hylidae). *South American Journal of Herpetology* 2:89–96 DOI 10.2994/1808-9798(2007)2[89:ACOFHF]2.0.CO;2.
- Orrico VGD, Dias IR, Marciano-Jr E. 2018.** Another new species of *Phyllodytes* (Anura: Hylidae) from the Atlantic Forest of northeastern Brazil. *Zootaxa* 4407:101–110 DOI 10.11646/zootaxa.4407.1.6.
- Palumbi S, Martin A, Romano S, McMillan WO, Stice L, Grabowski G. 2001.** The simple fool's guide to PCR. Version 2. Honolulu: University of Hawaii, 47. Available at <http://palumbi.stanford.edu/SimpleFoolsMaster.pdf>.
- Peixoto OL. 1995.** Associação de anuros a bromeliáceas na Mata Atlântica. *Revista Universidade Rural: Série Ciências da Vida* 17:75–83.
- Peixoto OL, Caramaschi U, Freire EMX. 2003.** Two new species of *Phyllodytes* (Anura: Hylidae) from the state of Alagoas, northeastern Brazil. *Herpetologica* 59:235–246 DOI 10.1655/0018-0831(2003)059[0235:TNSOPA]2.0.CO;2.
- Peixoto OL, Cruz CAG. 1988.** Descrição de duas espécies novas do gênero *Phyllodytes* Wagler (Amphibia, Anura, Hylidae). *Revista Brasileira de Biologia* 48:265–272.
- Pinkel D, Straume T, Gray JW. 1986.** Cytogenetic analysis using quantitative, high sensitivity, fluorescence hybridization. *Proceedings of the National Academy of Sciences of the United States of America* 83:2934–2938 DOI 10.1073/pnas.83.9.2934.
- Pyron RA. 2014.** Biogeographic analysis reveals ancient continental vicariance and recent oceanic dispersal in amphibians. *Systematic Biology* 63:779–797 DOI 10.1093/sysbio/syu042.
- Pyron RA, Wiens JJ. 2011.** A large-scale phylogeny of Amphibia including over 2,800 species, and a revised classification of extant frogs, salamanders, and caecilians. *Molecular Phylogenetics and Evolution* 61:543–583 DOI 10.1016/j.ympev.2011.06.012.
- Rambaut A, Drummond AJ, Xie D, Baele G, Suchard MA. 2018.** Posterior summarisation in Bayesian phylogenetics using Tracer 1.7. *Systematic Biology* 67(5):901–904.
- Roberto IJ, Ávila RW. 2013.** The advertisement call of *Phyllodytes gyrinaethes* Peixoto, Caramaschi & Freire, 2003 (Anura, Hylidae). *Zootaxa* 3669:193–196 DOI 10.11646/Zootaxa.3669.2.13.
- Rodrigues MT, Teixeira M, Recoder RS, Vechio F, Damasceno R, Pellegrino KCM. 2013.** A new species of *Leposoma* (Squamata: Gymnophthalmidae) with four fingers from the Atlantic Forest central corridor in Bahia, Brazil. *Zootaxa* 3635:459–475 DOI 10.11646/zootaxa.3635.4.7.
- Ron SR, Venegas PJ, Ortega-Andrade HM, Gagliardi-Urrutia G, Salerno PE. 2016.** Systematics of *Ecnomihyla tuberculosa* with the description of a new species and comments on the taxonomy of *Trachycephalus typhonius* (Anura, Hylidae). *Zookeys* 630:115–154 DOI 10.3897/zookeys.630.9298.
- Savage JM, Heyer WR. 1967.** Variation and distribution in the tree frog genus *Phyllomedusa* in Costa Rica, central America. *Beitrag zur Neotropischen Fauna* 5:111–131 DOI 10.1080/01650526709360400.
- Savage JM, Heyer WR. 1997.** Digital webbing formulae for anurans: a refinement. *Herpetological Review* 28:131.

- Simon JE, Gasparini JL. 2003.** Descrição da vocalização de *Phyllodytes kautskyi* Peixoto e Cruz, 1988 (Amphibia, Anura, Hylidae). *Boletim do Museu de Biologia Mello Leitão* **16**:47–54.
- Sumner AT. 1972.** A simple technique for demonstrating centromeric heterochromatin. *Experimental Cell Research* **75**:304–306 DOI [10.1016/0014-4827\(72\)90558-7](https://doi.org/10.1016/0014-4827(72)90558-7).
- Tamura K, Stecher G, Peterson D, Filipowski A, Kumar S. 2013.** MEGA6: molecular evolutionary genetics analysis version 6.0. *Molecular Biology and Evolution* **30**:2725–2729.
- Teixeira-Jr M, Vechio FD, Recoder RS, Carnaval ACO, Strangas M, Damasceno RP, Sena MA, Rodrigues MT. 2012.** Two new species of marsupial tree-frogs genus *Gastrotheca* Fitzinger, 1843 (Anura, Hemiphysalidae) from the Brazilian Atlantic Forest. *Zootaxa* **3437**:1–23 DOI [10.11646/zootaxa.3437.1.1](https://doi.org/10.11646/zootaxa.3437.1.1).
- Trueb L. 1973.** Bones, frogs, and evolution. In: Vial JL, ed. *Evolutionary biology of the anurans. Contemporary research on major problems*. Columbia: University of Missouri Press, 65–132.
- Vörös J, Dias IR, Solé M. 2017.** A new species of *Phyllodytes* (Anura: Hylidae) from the Atlantic Rainforest of Southern Bahia, Brazil. *Zootaxa* **4337**:584–594 DOI [10.11646/zootaxa.4337.4.9](https://doi.org/10.11646/zootaxa.4337.4.9).
- Weygoldt P. 1981.** Beobachtungen zur Fortpflanzungsbiologie von *Phyllodytes luteolus* (Wied, 1824) im Terrarium (Amphibia:Salientia: Hylidae). *Salamandra* **17**:1–11.
- Wiens JJ, Kuczynski CA, Hua X, Moen DS. 2010.** An expanded phylogeny of treefrogs (Hylidae) based on nuclear and mitochondrial sequence data. *Molecular Phylogenetics and Evolution* **55**:871–882 DOI [10.1016/j.ympev.2010.03.013](https://doi.org/10.1016/j.ympev.2010.03.013).